Digest Journal of Nanomaterials and Biostructures Vol. 19, No. 3, July -September 2024, p. 1147 - 1157

SRIM simulation of hydrogen ions interaction with bismuth oxide nanoparticles doped with rare earth elements

R. Alhathlool, M. H. Eisa*
Department of Physics, College of Science, Imam Mohammad Ibn Saud Islamic University (IMSIU), Riyadh 13318, Saudi Arabia

Simulation methods have received much attention across various fields in recent years. The rare-earth lutetium tantalate ($LuTaO_4$) doped "Bismuth Oxide (Bi_2O_3) thin films were deposited onto polymer substrates using a SRIM program." The SRIM program was used to calculate some physical characteristics of Bi_2O_3 films at energies between 1.0 MeV and 20 MeV. The "electronic and nuclear stopping powers" of $LuTaO_4$, Bi_2O_3, $C_{10}H_8O_4$, and $LuTaO_4$/ Bi_2O_3/$C_{10}H_8O_4$ samples were investigated. These findings show that rare earth doping may improve the performance of composite materials. The interaction of ion beams with matter can result in a wide variety of phenomena. The deposition of Bi_2O_3 films doped with $LuTaO_4$ on $C_{10}H_8O_4$ led to changes in the "electronic and nuclear stopping powers" and range in the materials. Published data were compared with the results obtained and the calculations parameters were provided.

(Received June 1, 2024; Accepted August 1, 2024)

Keywords: Stopping power, Bismuth oxide, Lutetium tantalite, SRIM, Polymer

1. Introduction

Alpha particles, deuterons, and protons significantly impact matter. Short-range nuclear forces interact with protons and alpha particles. As energy declines, charged-particles lose their velocity. In both ionization and excitation process, heavy charged-particles lose their energy. Heavy charged particles transfer less energy when they collide [1].

Thus, highly charged particles travel in almost straight lines in matter, losing energy from atom electron collisions. Low-velocity nuclear collisions lose less energy to heavy charged particles [1]. Depending on the kind and their energy, rapid particles penetrate materials differently [2]. To predict beam losses in systems requires understanding the interactions between proton or particle with matter. Because of its scientific importance, energetic charged particle-matter interactions have been widely studied experimentally and theoretically. This contact involves fast ions losing energy. This relationship is a crucial for "microelectronics, materials science, nuclear and plasma physics, radiation detectors, cancer therapy, and space exploration" [3].

For decades, several sectors have studied charged particle penetration through the soft or hard targets. Protons interact with matter through Coulomb interactions of protons-electrons, inelastic Coulomb scattering of protons-nuclei, and non-elastic nuclear interactions of protons-atoms. Inelastic Coulomb interaction dominates [4]. Thus, radiation energy absorption and attenuation must be understood. Ion beams like hydrogen (H) and helium (He) have never been stopped in bismuth oxide films [5, 6]. Many scholars have studied the proton theory of stopping power and heavier ions [4, 5]. The transport of hydrogen ions (protons) via bismuth oxide films must also be studied due to their potential applications. It is essential to know "the stopping power and inelastic mean free path (IMFP) of protons at various energies." Protons lose energy in three ways when they interact with materials [4]. Incident particle energy ranges from <0.5MeV to extremely high. Coulomb forces also deplete protons.

Heavy metal oxides are semiconductors and are used as sensing materials, particularly for gas detection. Bismuth oxide (Bi_2O_3) is a popular heavy metal oxide [7] with several applications due to its apparent activity. Bismuth oxide attracts interest "due to its exceptional optical and

* Corresponding author: mheisas@hotmail.com
https://doi.org/10.15251/DJNB.2024.193.1147

electrical properties, such as a large band gap, high refractive index, and high oxygen ion conductivity at high and medium temperatures." Bismuth oxide has excellent dielectric permittivity, photoconductivity, photoluminescence, and a narrow visible band gap [8-10]. Bi_2O_3 semiconductor is a good alternative due to its high density, big Zeff, and non-toxicity.

Bismuth oxide has six polymorphs: "monoclinic, tetragonal, body-centered cubic, orthorhombic, face-centered cubic, and triclinic" [10]. Each phase has unique electrical, optical, photoelectrical features [10]. Doping bismuth oxide with rare earth elements improves its activity [11]. Due to their peculiar f electron orbital structure, rare earth ions may enhance photocatalytic abruption of photogenerated electron-hole pairs [12, 13]. However, rare-earth element-doped Bi_2O_3 thin films have been studied [14, 15]. Lutetium tantalate ($LuTaO_4$) is a promising host lattice for luminous materials, especially for x-ray and gamma-ray excitation. Lutetium compounds are increasingly used for this.

Substrates have been stabilized and deposited many times [16]. Thus, thin films were developed to integrate high-performance oxides into affordable, flexible substrates. Paper, aluminum foil, PET (polyethylene terephthalate), PEN (polyethylene naphthalate), MYLAR, Transphan, and polycarbonate are flexible substrates. Polyimide (PI) and polyethylene terephthalate (PET) are commercial flexible substrates [17]. Modern technology uses poly (ethylene terephthalate) (PET) because of its outstanding qualities. Chemical vapor deposition, sputtering, electrodeposition, electrophoretic deposition, sol gel techniques, and pulse laser deposition (PLD) are the methods commonly used for synthesizing Bi_2O_3 thin films on substrates [18-23]. However, proton ion beam-based Bi_2O_3 films doped with Lutetium tantalate deposited on PET using SRIM simulation code have not been reported. Monte Carlo simulation code SRIM [4] is a software designed for the study of ion stopping power and range. Also, the field of thin film deposition and its specific applications are highly specialized, and up-to-date experimental data may not be readily available.

This work employ simulation code SRIM 2013 for calculating the projected range, energy loss, longitudinal straggling, phonons, and ionization of ion beam in Bi_2O_3 (SP1), $LuTaO_4$ (SP2), $C_5H_4O_2$ or PET (SP3), $LuTaO_4$ doped Bi_2O_3 (SP_4), and $LuTaO_4$ doped Bi_2O_3 deposited on PET substrates (SP5).

2. Materials and methods

2.1. The preparation of Bi_2O_3 films

SRIM code was used for the deposition of $LuTaO_4$-doped Bi_2O_3 films on $C5H_4O_2$. This study's materials were supplied by Sigma-Aldrich. Figure 1 shows the deposition geometry schematic. Lutetium tantalate ($LuTaO_4$) is the dopant. 9.81 g/cm^3. PET substrate is ($C_{10}H_8O_4$) n or $C5H_4O_2$ (PET). PET has 1.397 g/cm^3, n=1.640, A/Z=1.915, and I=73.2 eV. 0.60 dl/g viscosity and 250°C melting point. PET films received $LuTaO_4$-doped Bi_2O_3 films. Table 1 shows the different samples with their chemical formula.

Table 1. Chemical formula of the samples.

Material	Chemical Formula
Bismuth oxide	Bi_2O_3
Lutetium tantalite	LuTaO4
Polyethylene terephthalate (PET)	$C_{10}H_8O_4$
Lutetium tantalate doped-bismuth oxide	LuTaO4/ Bi2O3
Lutetium tantalate doped-bismuth oxide/PET	LuTaO4/Bi_2O_3/ $C_5H_4O_2$

2.2. Theoretical details

There are several protocols that are designed to facilitate the movement of hydrogen ions within composite materials. One of them is the SRIM code [24], which operates on Linux, Mac

OS, and Windows. Ion-solid interaction theories have advanced substantially in recent years. Monte-Carlo simulation of ion-solid interaction is popular and it is based on SRIM, TRIM, TRIDYN, and SDTrimSP [24–25]. The SRIM code is a computer program commonly used for ion beam analysis and ion implantation. It is used to simulate the behavior of ions in matter, including their energy loss, range, and straggling.

The SRIM provides a comprehensive set of models and algorithms to calculate the interactions of ions with solids, liquids, and gases. It takes into account various physical processes, such as nuclear stopping, electronic stopping, multiple scattering, and straggling [3]. To use the SRIM code, the following information about the ion species must be provided: energy, the target material, and the desired output parameters. After the information is provided, the program then performs simulations and provides detailed results on the ion's behavior within the target material [26].

Stopping power typically describes energy deposition (-dE/dx) [27]. SRIM is a popular program for determining stopping power and ion range in various materials [27]. Most calculations ignore radiation since it is small. There must be other ways to determine how far a particle can go in matter than ionization energy. Charged particle stopping power (SP) and energy dissipation via matter have garnered attention for years due to their diverse uses. Bethe-Bloch equation gives the formula of the stopping power for the heavy charged particles, like protons interacting with a material medium. As charged particles move through a medium, the Bethe-Bloch equation approximates their energy loss. Stopping energy refers to the energy loss per unit path length.

2.3. Stopping power

The term "stopping power" (SP) is energy change (dE) per increase in distance (dx). The SP term has long been used in electron transport theories. Bethe [27] developed a famous formula for non-relativistic energy that expresses the SP term well over several years ago. The SP formula [27] for heavy charged particles like protons is given below,

$$\frac{dE}{dx} = 4\pi r_0^2 Z^2 \ \frac{mc^2}{\beta^2} NZ \left[\ln\left(\frac{2mc^2}{I}\beta^2\gamma^2\right) - \beta^2\right] \tag{1}$$

where, "(dE/dx) is the particle stopping power measured in MeV/m, r_0 is the classical electron radius of 2.818×10^{-15}m, **z** the particle charge (**z** equals to *1* for proton, deuterium, beta β^-, beta ß $^+$ and z = 2 for alpha α), and mc^2 is the electron rest energy = 0.511 MeV." Thus, "*N* is the number of atoms per m^3 in the absorber material through which the charged particle travels ($N = \rho\ (N_A/A)$), where $\boldsymbol{\rho}$ is the absorber density in units of g/cm^3, Avogadro's number N_A is 6.022×10^{23} atoms per mol, *A* and *Z* are the atomic weight and atomic number, respectively of the absorber, $\gamma = (T+mc^2)/mc^2 = 1/\sqrt{\mathbf{1}-\boldsymbol{\beta}^{\mathbf{2}}}$."

Consequently, "*T* is the particle kinetic energy in MeV and *M* the particle rest mass (e.g., proton = 938.2 MeV/c^2) and *β* is the relative phase velocity. Here, I, represents the mean excitation potential in units of eV". Hence, it is given by the equation below,

$$\boldsymbol{I = \left(9.76 + 58.8\, Z^{-1.19}\right)Z} \tag{2}$$

In this case, Z > 12 and it constitutes "pure elements' according to [5].

Consequently, "energy, I⟩ must be calculated according to Bethe theory," especially when it involves a compound or mixture of elements. Thus, the "mean excitation" is described as:

$$< I >= \ exp\left\{\frac{\left[\sum_j w_j (z_j/A_j)\right] \ln I_j}{\sum_j w_j (z_j/A_j)}\right\} \tag{3}$$

Here, "w_j, Z_j, A_j, and I_j are the weight fraction, atomic number, atomic weight, and mean excitation energy, respectively, of the jth element." There are three types of stopping power:

collisional, radiative, and electronic. Collision stopping power results from Coulombic interactions with matter and is largely determined by particle speed and charge (z).

The kinetic energy loss per unit distance experienced by a charged particle is denoted as (−dEdx); conventionally, it is regarded as "stopping power" [2]. "The stopping power (dE/dx) of any particle is the average energy loss per unit path length of the particle" [5]. In addition, the energy dissipation and stopping power of charged particles through matter have been of great interest for several years, because of its wide areas of applications [5]. "Stopping power (-dE/dx) is defined as the energy lost by protons per unit path length. In this work, the mass stopping power concept [$\frac{1}{\rho}$(-dE/dx)] is adopted, which is density-independent. That means it depends on the material's property but not its density" [3].

$$\left(\frac{-dE}{dx}\right)_{Compound} = \sum W_i \left(\frac{dE}{dx}\right)_i \tag{4}$$

where, "w_i is the fraction by weight and $(dE/dx)_i$ is the mass stopping power of the constituent. Beth formula for a proton particle is given by [2]":

$$\frac{-dE}{dx} = \frac{4\pi n Z^2 k_0^2 \ Z^4}{m_0 V^2} \ ln\left(\frac{2m_0 V^2}{I}\right) \tag{5}$$

where "z is the charge of incoming particle, n is the number of electrons per unit volume in the stopping material, m_o is the rest mass of the electron, V is velocity of the particle, e is electron charge. The constant Ko is equal to $1/4\pi\ \varepsilon_o$ and I is a mean excitation energy of the medium. The stopping power was determined using Ziegler's equation for low and high energies." In the target atom, the ion can lose energy through "(i) excitation or ionization of the electrons (electronic energy loss), (ii) elastic collisions with the nuclei of target atoms (nuclear energy loss), and (iii) radiative emission." Thus, the total stopping power can be divided into three parts:

$$S_{Total} = S_{Electronic} + S_{Nuclear} + S_{Radiative} \tag{6}$$

or

$$\left(-\frac{dE}{dx}\right)_T = \left(-\frac{dE}{dx}\right)_e + \left(-\frac{dE}{dx}\right)_n + \left(-\frac{dE}{dx}\right)_r \tag{7}$$

In the presence of projectile energies below, the absolute speed of light $S_{radiative}$ is ignored. For proton and other heavy charged particle energies between 2.0 and 10.0MeV, the total stopping power is the sum of the two components:

$$\left(\frac{dE}{dx}\right)_{Total} = \left(\frac{dE}{dx}\right)_{collision} + \left(\frac{dE}{dx}\right)_{radiative} \tag{8}$$

where, $\left(\frac{dE}{dx}\right)_c$ is the "collision stopping power" and $\left(\frac{dE}{dx}\right)_r$ is the "radiative stopping power." The calculation of the radiative stopping power is complex and few efforts have been made along this line.

3.2 Nuclear energy and electronic loss calculations

Electronic energy loss occurs when an ion is ionized or excited by a coupling interaction with an atom of the target, resulting in the loss of energy. Despite the attention that has been given to radiation damage from nuclear stopping, electronic stopping still loses most ion energy. There are several theoretical models and computational methods available to calculate electronic energy

loss in materials. Charged particles interact with bound electrons in a complicated fashion. Thus, electrons in the target and energetic ion can collide elastically with projectiles and be stimulated or ionized [5]. An energetic ion loses electronic energy (Se):

$$S_e = \left(-\frac{dE}{dx}\right)_e = \frac{4e^4 Z_p^2 Z_t N_t}{mev^2}\left[ln\left(\frac{2m_e v^2}{I}\right) - ln\left(1-\frac{v^2}{c^2}\right) - \frac{v^2}{c^2}\right] \quad (9)$$

$$\left(\frac{dE}{dx}\right)_e = NZ_2\,\pi\,\frac{Z_1^2 e^2 m_1}{E\ m_e}\ln\left(\frac{\gamma E}{\bar{I}}\right) \quad (10)$$

where, "γ is the kinematic factor $4m_1m_2/(m_1+m_2)^2$ and $\bar{I}$ is the average ionization energy. Equation 10 arises only from the analysis of elastic collisions for electronic stopping at high energies. At low projectile energies, the ion is close to neutral and the conduction electrons contribute more to the electronic energy loss." Here, "$\mathbf{Z}_p$, **e** and **v** are the atomic number of the projectile ions, charge and velocity, respectively. The target atom's number density and atomic number are N_t and Z_t. The electron rest mass, the electron elementary charge and ionization or target excitation target are given as m_e; *e* and ***I***, respectively."

The nuclear energy loss refers to the reduction or dissipation of energy from a nuclear system. It can occur through various processes, including radioactive decay, nuclear reactions, and energy conversion mechanisms. The nuclear energy loss occurs as atoms in the medium are displaced by the incident ion when they interact with the Coulomb field of the target nucleus [24]. Loss of nuclear energy (Sn) can be expressed as shown below [24]:

$$S_n = \left(-\frac{dE}{dx}\right)_n = N\frac{\pi^2}{2}Z_1 Z_2 e^2 \alpha \frac{M_1}{M_1+M_2} \quad (11)$$

where, "Z_1e denotes the projectile nuclear charge; Z_2e represents the target nuclear charge; **I,** is the target average excitation; and N_A refers to the Avogadro number." The rule says that "the mass stopping power for the substance containing several elements is taken to be equal to the weighted sum of the mass stopping power of the constituent." This is expressed as:

$$\left(\frac{-dE}{\rho dx}\right)_{Compound} = \frac{1}{M}\sum N_i A_i \left(\frac{-dE}{\rho dx}\right)_i \quad (12)$$

Here, "*M* is the molecular weight of the compound medium containing *Ni* atoms of atomic weight *Ai*." For instance, the stopping power for Bi_2O_3 compound is expressed below:

$$\frac{-dE}{\rho dx} = \frac{1}{M}\left[2\,N_{Bi}\,A_{Bi}\left(\frac{-dE}{\rho dx}\right)_{Bi} + 3\,N_O\,A_O\left(\frac{-dE}{\rho dx}\right)_O\right] \quad (13)$$

$$\frac{-dE}{\rho dx} = \frac{1}{(465.96)}\left[2(208.9804)\left(\frac{-dE}{\rho dx}\right)_{Bi} + 3\,(15.999)\left(\frac{-dE}{\rho dx}\right)_O\right]$$

$$\frac{-dE}{\rho dx} = \left[(0.8969885827)\left(\frac{-dE}{\rho dx}\right)_{Bi} + (0.1030066959)\left(\frac{-dE}{\rho dx}\right)_O\right] \quad (15)$$

3.3 Ions range calculations

The term "ions range" refers to the distance that ions can travel through a material before losing their energy and coming to a stop. The ions range is an important parameter in materials science and is used to study various phenomena, such as ion implantation, radiation damage, and electronic stopping power **[27].** The ions range in a material can be calculated using theoretical

models or empirical formulas. The most commonly used model for calculating ions range in materials is "the Stopping and Range of Ions in Matter (SRIM) program." In estimating the ranges of ions, several factors are considered, such as the ion energy, the ion type, and the medium through which the ions are traveling. The range of ions can be estimated using empirical formulas or simulation techniques.

To calculate the ions range using SRIM, the following information must be provided: (i) The type of ion of interest, such as hydrogen (H+), helium (He+), or heavier ions like oxygen (O+) or silicon (Si+). (ii) Ion energy: The initial energy of the ion before it enters the material. This is typically specified in units of electron volts (eV) or kiloelectron volts (keV). (iii) Target material: The material through which the ion will travel. This could be a single element or a compound. (iv) Target thickness: The thickness of the material the ion will traverse. This is typically specified in units of nano-meters (nm) or micro-meters (μm). By providing these inputs to the SRIM program, it calculates the ions range by considering various interaction mechanisms between the ion and the target material, such as elastic scattering, inelastic scattering, and nuclear collisions. A charge particle's range (R) and stopping power (S) in a specific target are related to the formula,

$$R = \int_{E_1}^{0} \left(\frac{dE}{\rho dx}\right)^{-1} dE = \int_{0}^{E_1} \left(\frac{1}{S}\right) dE \tag{15}$$

The range of a proton in a compound refers to the distance over which the influence of a proton extends within that compound. It is important to note that the range of a proton can vary depending on the specific compound and its chemical environment. A proton's range in matter is calculated by simple numerical integration of its reciprocal. Charged particles in all constituent elements of a compound material are described below:

$$R_{Compound} = R_C = \frac{M_C}{\sum n_i \left(\frac{A_i}{R_i}\right)} \tag{16}$$

where, "the range of element i is R_i, the number of atoms of element i is n_i, the atomic weight of element i is A_i, and the molecular weight of compound is M_c. This formula has also been used by different authors to present the range of proton in several compounds." The compound Bi_2O_3 can be described by equation (16)

$$R_C = \frac{465.96}{2\frac{208.9804}{R(Bi)} + 3\frac{15.999}{R(O)}} = \frac{465.96}{\frac{2[208.9804]R(O) + 3[15.999]R(Bi)}{R(Bi)R(O)}}$$

$$R_C = \frac{[465.96]R(Bi)R(O)}{2[208.9804]R(O) + 3[15.999]R(Bi)} = \frac{R(Bi)R(O)}{\frac{3[15.999]R(Bi)}{[465.96]} + \frac{2[208.9804]R(O)}{[465.96]}}$$

$$R_C = \frac{R(Bi)R(O)}{(0.1030066959)R(Bi) + (0.8969885827)R(O)}$$

The molecular weight (Mc) of the compound, Bi_2O_3 is 465.96 g/mol, the atomic weight (A_{Bi}) of bismuth element is 208.9804 u and the atomic weight (A_O) of oxygen element is 15.999 u. The experimental measurements of tabulated data, current computer codes, and stopping power compilations often show discrepancies. The SRIM 2013 simulation code is used to calculate energy losses, projected ranges, longitudinal straggling, phonons, and ionization of ion beams in SP1, SP2, SP3, SP4 and SP5 at energies of 0.01 to 20.0 MeV. The sample was then stimulated with detailed calculations and damage cascades' analysis.

The analysis considered collision cascade damage using 99000 ions. The information of the "ions and targets used in the SRIM analysis of the samples $LuTaO_4$, Bi_2O_3, PET, $LuTaO_4/Bi_2O_3$ and $LuTaO_4/Bi_2O_3$/PET" is summarized in Tables 2 to 8. The $LuTaO_4$ composite is composed of SRIM inputs, such as lutetium (Lu), tantalate (Ta) and oxygen (O_4) in percentages.

For $LuTaO_4$ composite, the compound below were added to make up the percentage composition: SRIM inputs, Oxygen (O_4), lutetium (Lu), and tantalate (Ta).

Table 2. Report of hydrogen ion employed in SRIM calculations.

Element	Atomic Number	Mass (amu)	Ion Energy Range (MeV)	
			Lowest	Highest
Hydrogen	1	1.008	1.000	20.000

Table 3. $LuTaO_4$ "elemental composition used in SRIM calculations, density," $\rho = 5.3577\ g/cm^3 = 4.6100\times10^{22}\ atoms/\ cm^3$.

Element	Atomic Number	Weight (amu)	Stoich.	Atom%
Lutetium, Lu	71	174.97	1	016.67
Tantalum, Ta	73	180.95	1	016.67
Oxygen, O	8	15.999	4	66.67

Table 4. Bi_2O_3 "Elemental composition used in SRIM calculations, density," $\rho = 04.77560\ g/cm^3$.

Element	Atomic Number	Weight (amu)	Stoich	Atom%
Bismuth, Bi	83	208.98	2	40.00
Oxygen, O	8	15.999	3	60.00

Table 5. $C_{10}H_8O_4$: "Elemental composition used in SRIM calculations, density," $\rho = 1.30936\ g/cm^3$.

Element	Atomic Number	Weight (amu)	Stoich	Atom%
Hydrogen, H	1	1.008	8	36.36
Carbon, C	6	12.011	10	45.45
Oxygen, O	8	15.999	4	18.18

Table 6. $LuTaO_4/Bi_2O_3$ films "elemental composition used in SRIM calculations, density," $\rho = 4.14516 g/cm^3$.

Element	Atomic Number	Weight (amu)	Stoich	Atom%
Lutetium, Lu	71	174.97	1	09.09
Tantalum, Ta	73	180.95	1	09.09
Oxygen, O	8	15.999	4	36.36
Bismuth, Bi	83	208.98	2	18.18
Oxygen, O	8	15.999	3	27.27

Table 7. $LuTaO_4/Bi_2O_3/C_{10}H_8O_4$ films "elemental composition used in SRIM calculations, density," $\rho = 2.43839 g/cm^3$.

Element	Atomic Number	Weight (amu)	Stoich	Atom%
Lutetium, Lu	71	174.97	1	03.03
Tantalum, Ta	73	180.95	1	03.03
Oxygen, O	8	15.999	4	12.12
Bismuth, Bi	83	208.98	2	06.06
Oxygen, O	8	15.999	3	09.09
Carbon, C	6	12.011	8	24.24
Hydrogen, H	1	1.008	10	30.30
Oxygen, O	8	15.999	4	12.12

Table 8. "Stopping powers, ion range, and straggling" in $LuTaO_4$, Bi_2O_3, $C_{10}H_8O_4$, and $LuTaO_4/Bi_2O_3$ /$C_{10}H_8O_4$ for 1.0 to 20.0 MeV Hydrogen –ions.

Parameter	$LuTaO_4$	Bi_2O_3	$LuTaO_4/Bi_2O_3/C_{10}H_8O_4$
Projected Ion Range (nm)	14200 to 1610000	16880 to 1980000	0.1138 to 0.0223
Longitudinal Straggling (nm)	1290 to 85840	1670 to 114710	0.001799 to 0.0000111
Lateral Straggling (nm)	1980 to 147650	2540 to 204750	0.00000016 to 0.00074579
Stopping power-electronic (MeV/(gm/cm^2)	0.08754 to 0.0134	0.0773 to 0.01228	0.0000001108 to 0.00004485
Stopping power-nuclear (MeV/(gm/cm^2)	0.00007553 to 0.000005903	0.0000675 to 0.000005387	0.0000000911 to 0.00007321

4. Results and discussion

4.1. The findings of the loss electronic and nuclear energy

When energetic particles like ions or electrons interact with matter, electronic and nuclear energy loss occurs. Using the empirical relation, the stopping powers and range are calculated from 1.0 Mev to 20 MeV proton energy for $LuTaO_4$, Bi_2O_3, $C_{10}H_8O_4$, and $LuTaO_4/Bi_2O_3$ /$C_{10}H_8O_4$ materials. For the light ions, such as hydrogen (H), the estimation of the electronic "stopping power" is done using equation (9). The "stopping power" results calculated by the empirical formula are depicted in Figures 1 to 3, along with available theoretical values. Table 9 shows the stopping power in MeVcm^2/g for $LuTaO_4$, Bi_2O_3, $C_{10}H_8O_4$, and $LuTaO_4/Bi_2O_3/C_{10}H_8O_4$ for proton energy 1MeV to 20MeV. The S_e values of $LuTaO_4$ are given at 0.01340 to 0.08754 MeV/gcm^2, whereas the S_n values of $LuTaO_4$ are given at 0.000005903 to 0.00007553MeV/g cm^2.

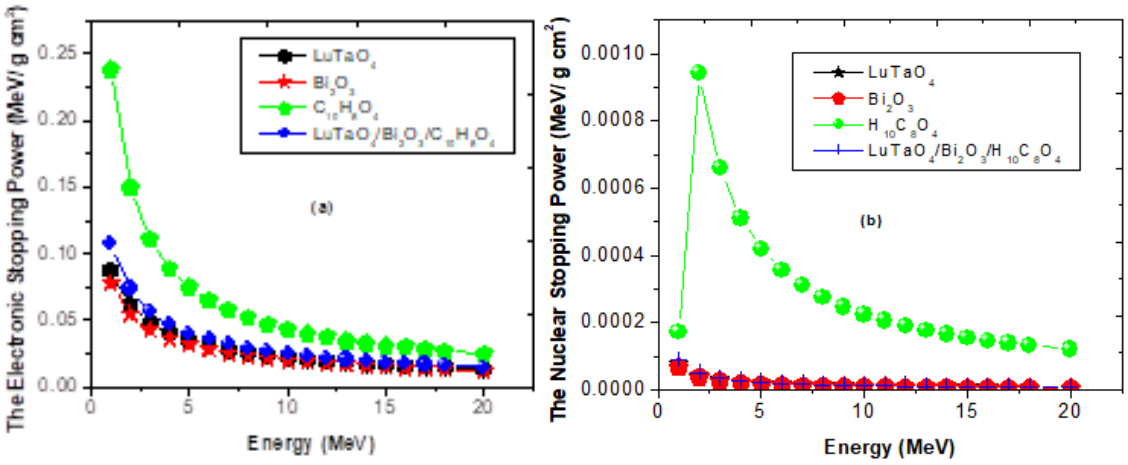

Fig. 1. Proton energy in MeV and the stopping power values for LuTaO4, Bi_2O_3, $C_{10}H_8O_4$, and $LuTaO_4/Bi_2O_3/ C_5H_4O_2$ in MeV/g/cm², "(a) electronic stopping power and (b) Nuclear stopping power."

The density of pure bismuth oxide (Bi_2O_3) is around 8.9 g/cm³. Lutetium tantalate ($LuTaO_4$) doping may slightly change density, although it should stay within a same range. The Se value of $LuTaO_4$ is typically higher for light ions and decreases as the ion's velocity increases. The electronic "stopping power" displays a steep down with increasing energy, as shown in Figure 1 (a), which compares the electronic stopping power for LuTaO4, Bi_2O_3, $C_{10}H_8O_4$, and $LuTaO_4/Bi_2O_3/ C_5H_4O_2$ in MeV/g/cm². The "electronic stopping power" of LuTaO4, Bi2O3, C10H8O4 compound material is commonly known as phthalic acid), or the composite LuTaO4/Bi2O3/C5H4O2.

However, depending on the incident particle, such as electrons, protons, or heavier ions, the “electronic stopping power” varies dramatically. Also, “the electronic stopping power can be influenced by the energy of the incident particle, the density and composition of the material, and other factors, such as temperature and crystal structure” [28]. The S_n value of the $LuTaO_4$ is related to the interactions between the incident ion and the atomic nuclei within the target material. It is generally less significant than electronic stopping power for light ions, but it becomes more important as the ion's mass and velocity increase. The changes observed in the “electronic and nuclear stopping powers” can have significant implications for the behavior of the doped film-substrate system. These alterations can influence the ion penetration depth, energy distribution, and overall damage profile within the materials.

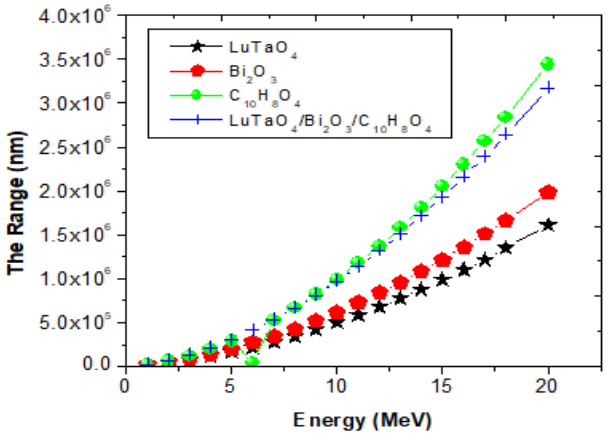

Fig. 2. Proton energy in MeV and the rang values for LuTaO4, Bi_2O_3, $C_{10}H_8O_4$, and LuTaO4/Bi_2O_3/ $C_5H_4O_2$ in MeV/g/cm².

Ion projected range and longitudinal straggling are important parameters to consider when studying the interaction of ions with materials. By simulating the ion's interactions within the $LuTaO_4$: Bismuth Oxide thin film using the SRIM program, the projected range for the specific ion species and energy of interest can be obtained.

The ion projected range and longitudinal straggling for $LuTaO_4$ are 14200 to 1610000 nm and 1290 to 85840 nm, respectively. For Bi_2O_3, these values are 16880 to 1980000 nm and 1670 to 114710 nm, respectively. $C_{10}H_8O_4$ has an ion projected range of 20420 to 3440000 nm and longitudinal straggling ranging from 885.4 to 137290 nm. The ion projected range and longitudinal straggling of $LuTaO_4$/Bi_2O_3 /$C_{10}H_8O_4$ are given at 24240 to 3170000 nm and 1850 to 160980 nm, respectively.

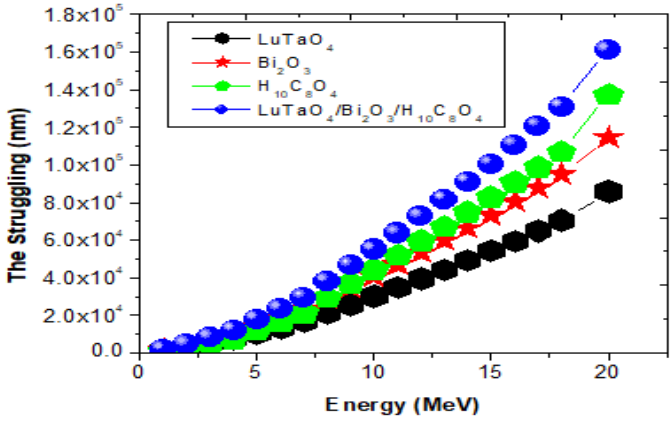

Fig. 3. Proton energy in MeV and the struggling values for $LuTaO_4$, Bi_2O_3, $C_{10}H_8O_4$, and LuTaO4/Bi_2O_3/ $C_5H_4O_2$ in MeV/g/cm².

5. Conclusions

In the present work, we comprehensively analyzed the effect of rare-earth ($LuTaO_4$) doping on the physical properties of bismuth oxide (Bi_2O_3) system and deposited it on $C_{10}H_8O_4$ substrates using the SRIM potential code. The investigation of the SRIM spectra confirmed that the rare earth-$LuTaO_4$ doped with Bi_2O_3 films on $C_{10}H_8O_4$ substrates resulted in alterations in the materials' "electronic and nuclear stopping powers". Doping rare-earth elements like lutetium (Lu) and tantalum (Ta) into the bismuth oxide system (LuTaO4) potentially modified its properties, enhancing its performance for specific applications. It can be used in the development of lasers, phosphors, scintillators, and other optical devices due to its ability to emit and absorb light in specific wavelength ranges.

Acknowledgements

The author gratefully acknowledges the assistance of numerous SRIM users and friends during various phases of this work. Special thanks are extended to colleagues for their support. This research has no grant number or external funding to report as it was privately funded by the authors.

References

[1]. J. E. Turner, Atoms, Radiation, and Radiation Protection, Wiley, New York, (1995)

[2] M. Nastasi, J. W. Mayer, J. K. Hirvonen, Ion-Solid Interactions: Fundamentals and Applications, Cambridge Solid State Science Series, Cambridge University Press, (1996); https://doi.org/10.1017/CBO9780511565007

[3] M. O. El- Ghossain, International Journal of Physics, 5(3), (2017) 92-98

[4] J. F. Ziegler, J. P. Biersack, U. Littmark, The stopping and range of ions in solids, Pergamon, New York, (1985); https://doi.org/10.1007/978-1-4615-8103-1_3

[5] J. F. Ziegler, Journal of Applied Physics 85, (1999) 1249-1272; https://doi.org/10.1063/1.369844

[6] E. Rauhala, N. P. Barradas, S. Fazinic, M. Mayer, E. Szilágyi, M. Thompson, Nucl. Instr. Meth. B 244 (2006) 436 – 456; https://doi.org/10.1016/j.nimb.2005.10.024

[7] H. J. Möller, Progress in Materials Science, Volume 35, Issues 3-4, (1991) PP. 205-418; https://doi.org/10.1016/0079-6425(91)90001-A

[8]. M.K.M. Ali, K. Ibrahim, O. S. Hamad, M. H. Eisa, M. G. Faraj, F. Azhari, Rom. J. Phys. 56, (2011) 730-741

[9] S. A. Knickerbocker, A. K. Kulkarni, J. Vac. Sci. Technol. A13 (3), (1995) 1048

[10] L. Hao, X. Diao, H. Xu, B. Gu, T. Wang, Appl. Surf. Sci. 254, (2008), 3504; https://doi.org/10.1016/j.apsusc.2007.11.063

[11] O. Tuna, Y. Selamet, G. Aygun, L. Ozyuzer, J. Phys. D: Appl. Phys. 43, (2010), 055402; https://doi.org/10.1088/0022-3727/43/5/055402

[12] S. Naseem, I. A. Rauf, K. Hussain, N. A. Malik, Thin Solid Films 156 (1988) 161; https://doi.org/10.1016/0040-6090(88)90291-X

[13] D. J. Seo and S. H. Park, Physica B, vol. 357, no. 3-4, (2005) pp. 420-427; https://doi.org/10.1016/j.physb.2004.12.008

[14] C. Liu, T. Mihara, T. Matsutani, T. Asanuma, M. Kiuchi, Solid State Commun.126, (2003), 509; https://doi.org/10.1016/S0038-1098(03)00237-0

[15] D. Ginley, B. Roy, A. Ode et al., Thin Solid Films, vol. 445, no. 2, (2003) pp. 193-198; https://doi.org/10.1016/j.tsf.2003.08.008

[16]. J. F. Ziegler, M. D. Ziegler, J. P. Biersack, Nucl. Inst. Meth. Phys. Res. B 268 (2010) 1818-

1823; https://doi.org/10.1016/j.nimb.2010.02.091
[17]. C. Bach, X. Dauchy, S. Etienne, Materials Science and Engineering 5, 012005 (2009); https://doi.org/10.1088/1757-899X/5/1/012005
[18] T. Takeyama, N. Takahashi, T. Nakamura, S. Itoh, Mat. Lett. 60, 2006, 1733; https://doi.org/10.1016/j.matlet.2005.12.006
[19] J. Morasch, S. Li, J. Brötz, W. Jaegermann, A. Klein, Phys. Status Solidi A 211, 2014, 93; https://doi.org/10.1002/pssa.201330216
[20] L.-C. Tien, Y-H. Liou, Surface and Coatings Technology, 265, 15 March (2015), Pages 1-6; https://doi.org/10.1016/j.surfcoat.2015.01.072
[21] X. Guo, X. Ming Li, C. Lai, W. Lin Li, D. Xiong Zhang, Z. Shu Xiong, Appl. Surf. Sci., (2015); https://doi.org/10.1016/j.apsusc.2015.01.034
[22] X. Xiaohong, Q. Wei, H. Weidong, J. Molecular Catalysis A: Chemical 261, 2007, 167; https://doi.org/10.1016/j.molcata.2006.08.016
[23] L. Leontie, M. Caraman, A. Visinoiu, G.I. Rusu, Thin Solid Films, 473, pp. 230-235, 2005; https://doi.org/10.1016/j.tsf.2004.07.061
[24] Juraj Hanžek, Pavo Dubcek, Stjepko Fazini, Kristina Tomi, Luketi, Marko Karlušic, Materials 2022, 15, 2110; https://doi.org/10.3390/ma15062110
[25] Mutke, A.; Schneider, R.; Bandelow, G. SDTrimSP-2D: Simulation of particles Bombarding on a Two-Dimensional Target (Version 2.0) (IPP 12/11); Max-Planck-Institut für Plasmaphysik: Garching, Germany, 2013. [Google Scholar].
[26] J. F. Ziegler, J.P. Biersack, M.D. Ziegler, Ion Straggle and TRIM: Output Files. In The Stopping and Range of Ions in Matter; Springer: Boston, MA, USA, 2008. [Google Scholar]
[27] M. H. Eisa, A. H. A. Alfedeel, Digest Journal of Nanomaterials and Biostructures, 15 (1), (2020), p. 59 – 65; https://doi.org/10.15251/DJNB.2020.151.59
[28]. S. J. Zinkle, Y. J. Matsukawa, Nucl. Mater. 2004, 329-333, 88-96; https://doi.org/10.1016/j.jnucmat.2004.04.298